Dalton Transactions

PAPER

View Article Online
View Journal | View Issue

Cite this: *Dalton Trans.*, 2015, **44**, 8617

An ionic liquid process for mercury removal from natural gas†

Mahpuzah Abai,[a,b] Martin P. Atkins,*[b] Amiruddin Hassan,[a] John D. Holbrey,*[b] Yongcheun Kuah,[a,b] Peter Nockemann,[b] Alexander A. Oliferenko,[b] Natalia V. Plechkova,[b] Syamzari Rafeen,[a,b] Adam A. Rahman,[a] Rafin Ramli,[a,b] Shahidah M. Shariff,[a] Kenneth R. Seddon,*[b] Geetha Srinivasan*[b] and Yiran Zou[b]

Received 23rd October 2014,
Accepted 11th February 2015

DOI: 10.1039/c4dt03273j

www.rsc.org/dalton

Efficient scrubbing of mercury vapour from natural gas streams has been demonstrated both in the laboratory and on an industrial scale, using chlorocuprate(II) ionic liquids impregnated on high surface area porous solid supports, resulting in the effective removal of mercury vapour from natural gas streams. This material has been commercialised for use within the petroleum gas production industry, and has currently been running continuously for three years on a natural gas plant in Malaysia. Here we report on the chemistry underlying this process, and demonstrate the transfer of this technology from gram to ton scale.

Introduction

Mercury is a natural component of the earth's crust, and through a number of natural and anthropogenic cycles is released into the environment as a toxic pollutant.[1] All forms of mercury *viz*. elemental mercury and oxidised, Hg(I) and Hg(II) are intrinsically toxic.[2] One of the main sources of environmental pollution by mercury is from fossil fuels, either during combustion of coal or emitted from natural gas.[3] Many natural gas fields contain mercury released from mercury-containing ores through secondary geothermal processes. Natural gas fields typically contain mercury, in either elemental or combinations of elemental and organometallic forms, in concentrations in the range <0.1–5000 μg m^{-3} depending on geographical location and geology. Although these concentrations are usually relatively low, for a typical gas processing plant treating 250 MMSCFD (million standard cubic feet per day = 28 300 m^3 d^{-1}) of natural gas, the cumulative quantities can be significant and can lead to problems through accumulation *via* condensation and amalgamation. High mercury concentrations in oil and gas production correlate with regions of high mercury emission to the environment (see Fig. 1).[4]

Mercury can be extremely corrosive, causing destructive damage to process equipment, particularly aluminium heat exchangers, through liquid metal embrittlement.[5] For example, an explosion in 1973 at the Skikda liquefied natural gas plant in Algeria led to 27 fatalities and financial losses of $1 billion due to catastrophic failure of an aluminium heat exchanger through reaction with mercury contaminants.[6]

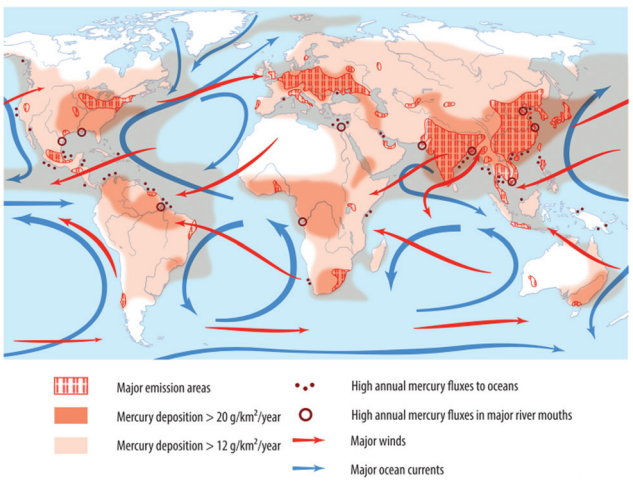

Fig. 1 Global mercury transport, indicating the major areas of emission (in red) taken from United Nations Environment Programme, Global Mercury Assessment.[4]

Mercury control and treatment within the oil and gas supply chain is increasingly recognised as important, both to protect equipment and personnel from deleterious exposure, and in order to comply with increasingly stringent discharge regulations. For natural gas processing, mercury control usually signifies the use of fixed-bed scrubbers containing a solid adsorbent that can capture mercury vapour either through adsorption, amalgamation, or oxidation followed by adsorption. The

[a]*PETRONAS Research Sdn. Bhd., Lot 3288 & 3289, Off Jalan Ayer Itam, Kawasan Institusi Bangi, 43000 Kajang Selangor, Malaysia*
[b]*QUILL, The Queen's University of Belfast, Belfast, BT9 5AG, UK.*
E-mail: quill@qub.ac.uk

†CCDC 1029551. For crystallographic data in CIF or other electronic format see DOI: 10.1039/c4dt03273j

Table 1 Various mercury removal systems for natural gas streams[7]

Active compound	Support/ medium	Fate of mercury
Sulfur	Carbon/ alumina	HgS
Metal sulfide	Carbon/ alumina	HgS
Silver	Zeolite	Ag–Hg amalgam
Thiol/oxidising agent/ chelating agent	Scavenger solution	Soluble Hg(II) compound
Metal oxide/sulfide	Metal oxide	HgO/HgS

most common approaches employ commercially available scrubbers, as shown in Table 1, incorporating sulfur, metal oxides/sulfides, or metals (particularly silver) as active agents on porous alumina, zeolite, or activated carbon supports.[7]

Sulfur-impregnated activated carbons are probably the most widely used adsorbents for mercury control within the gas industry. Impregnation of sulfur into activated carbons overcomes some of the slow kinetics of the reaction of mercury with elemental sulfur under ambient conditions. Vidić and co-workers have proposed that this is may be due to the involvement of sulfur allotropes with greater number reactive end groups.[8] However, activated carbons are not as mechanically robust as oxide supports such as alumina or silica, and therefore suffer from attrition which shortens their operational lifetimes.[7] Mercury capture from gas using copper(II) chloride impregnated on carbon as a 'chloride' source has been investigated,[9] however the resulting mercury(II) chloride was incompletely captured and leached under high pressure conditions.[10]

Ionic liquids[11] have also been explored for liquid/liquid partitioning of mercury, as mercury(II), from water,[12] initially using hydrophobic ionic liquids containing pendant sulfur ligands.[13] Subsequently, it was shown that mercury(II) can partition into unfunctionalised hydrophobic ionic liquids.[14,15]

The effective involatility of most ionic liquids means that gas–liquid contacting scenarios can be considered without contaminating process gas streams. Pinto and co-workers have reported the use of ionic liquids to capture elemental and oxidised mercury from combustion flue gases, combining the ionic liquid with permanganate(VII) as an oxidant.[16] Rogers and Holbrey[17] have suggested using ionic liquids containing perhalide anions for the oxidative dissolution of metals, and Sasson and co-workers[18] have reported using similar ionic liquid systems as liquid scrubbers to remove mercury from power-plant combustion gas. However, the corrosive nature of these highly oxidising ionic liquids (analogous to chlorine or bromine) to metals such as iron may place restrictions on their applicability.

Building on previous work developing ionic liquid approaches to oxidative dissolution,[19,20] and selective extraction and separations,[21] we considered whether ionic liquids[22] incorporating metal complexes might oxidise elemental mercury, leading to the formation of stable anionic mercurate(II) species. Such anions should then become integral components of a new, more complex, ionic liquid system,[23] which would also be non-volatile. Here, we report on the investigation of chlorocuprate(II)-based ionic liquids for the direct oxidation of elemental mercury,[24] and the use of these ionic liquids in a solid-supported ionic liquid phase (SILP)[25] for reactive capture of mercury from gas streams, which has led to the scale-up and deployment on industrial plants in Malaysia.[26]

Experimental

^{199}Hg NMR spectra were measured using a Bruker 500DRX spectrometer with a 1 M solution of $HgCl_2$ (Sigma Aldrich) in dmso-d_6 as an internal standard (−1501 ppm relative to $Hg(CH_3)_2$ and deuterium lock.[27] IR spectroscopy was carried out using a Perkin Elmer Spectrum 100 FT-IR spectrophotometer with a Universal diamond Attenuated Total Reflectance (ATR) top plate.

Mercury solubility in ionic liquids was measured by dissolving an accurately weighed sample of the ionic liquid phase (*ca.* 0.05 g) in water (10 cm^3), removing the small quantity of precipitate produced by filtration, and then diluting to 50 cm^3, followed by subsequent dilution of a 1 cm^3 aliquot to 50 cm^3. A sample (<50 μL) calculated to contain less than 1000 ng mercury was then analysed for mercury using a Milestone DMA-80 direct mercury analyser. Based on the sample size, initial mass of ionic liquid used for the contact test, and mercury content determined, the wt% of water soluble mercury present in the ionic liquid was calculated.

Mercury capture from the carrier gas by SILPs was tested using an accelerated breakthrough test rig constructed in-house, incorporating a mercury generator and Sir Galahad analyser (PS Analytical). SILPs (and commercial activated carbons for comparison) were crushed and sieved using a 300–500 μm mesh. Adsorbents (30–100 mg) were packed into a thermostated glass column of diameter 1 mm. Mercury removal from test gas streams (nitrogen and methane) was examined using a high flow rate (600 cm^3 min^{-1}) and high mercury content (2000 ng l^{-1}) in the carrier gas; the outlet mercury concentration was monitored continuously.

Crystallography

A suitable crystal of $[N_{4\ 4\ 4\ 1}]_2[Cu_2Cl_6]$ was selected and measured on a Rigaku Saturn724+ (2 × 2 bin mode) diffractometer. The crystal was kept at 120.0 K during data collection. Using Olex2,[28] the structure was solved with the ShelXS[29] structure solution program using Direct Methods and refined with the ShelXL refinement package using Least Squares minimisation. Crystal Data for $C_{13}H_{30}Cl_3CuN$ (M = 370.27 g mol^{-1}): monoclinic, space group $P2_1/n$ (no. 14), a = 9.2771(4) Å, b = 15.6784(5) Å, c = 12.5521(5) Å, β = 100.016(2)°, V = 1797.88(12) Å^3, Z = 4, T = 120.0 K, μ(MoK$_\alpha$) = 1.647 mm^{-1}, D_{calc} = 1.368 g cm^{-3}, 21 158 reflections measured (5.98° ≤ 2Θ ≤ 54.96°), 4122 unique (R_{int} = 0.0469, R_σ = 0.0382) which were used in all calculations. The final R_1 was 0.0377 (>2σ(I)) and wR_2 was 0.0951 (all data).

Results and discussion

Synthesis and characterisation of copper(II) ionic liquids

Chlorocuprate(II) ionic liquids were prepared by combining 1-butyl-3-methylimidazolium chloride ([C_4mim]Cl), 1-ethyl-3-methylimidazolium chloride ([C_2mim]Cl), or tributylmethylammonium chloride ([$N_{4\,4\,4\,1}$]Cl, (*ex.* Sigma Aldrich) with copper(II) chloride (either anhydrous or dihydrate, *ex.* Sigma Aldrich) in methanol in either a 1 : 1 or 2 : 1 molar ratio, followed by solvent removal under reduced pressure, and then *in vacuo* at 80 °C. It is convenient to define the ionic liquid systems by the mole fraction χ_{CuCl_2}, which is defined by $\chi_{CuCl_2} = n_i/(n_i + n_c)$, where n_i is the number of moles of $CuCl_2$ and n_c is the number of moles of cation. The resulting ionic liquids formed as dark yellow-brown liquids which, in all cases, slowly solidified on standing at room temperature. Additionally, a 1 : 2 : 1 cholinium chloride–diethylene glycol–$CuCl_2{\cdot}2H_2O$ deep eutectic[30] was prepared as a dark green liquid. The ionic liquids were characterised by DSC, TGA, microanalysis, electronic absorption and vibrational spectroscopy, Karl Fischer titration and surface analysis by SEM/EDAX.

Small single crystals were isolated from the bulk solidified $[N_{4\,4\,4\,1}]_2[Cu_2Cl_6]$ ionic liquid (1 : 1 $CuCl_2$: [$N_{4\,4\,4\,1}$]Cl), and analysed by X-ray crystallography. The structure confirmed the presence of a dimeric copper(II) dianion with four-coordinate copper centres separated by 3.33 Å (Fig. 2). Li *et al.*[31] have reported that [C_2mim]Cl/copper(II) chloride mixtures form $[CuCl_4]^{2-}$ chlorocuprate(II) anions even in the presence of substantial concentrations of water. It was thus not anticipated that copper speciation would differ in ionic liquids formed with anhydrous or hydrated copper(II) chloride. Crystal structures of many chlorocuprate(II) salts with a variety of organic cations have been previously reported,[32] and are dominated by salts of the discrete tetrachlorocuprate(II) anion, which can vary in structure from tetrahedral to square planar, with many intermediate geometries.

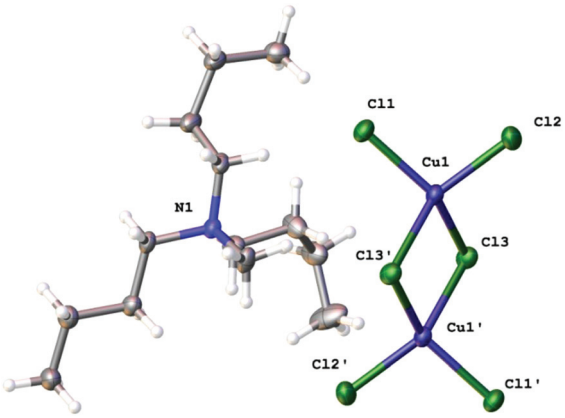

Fig. 2 Cation and anion within the unit cell of $[N_{4\,4\,4\,1}]_2[Cu_2Cl_6]$; $\bar{d}(CuCl)_t$ = 2.19, $\bar{d}(CuCl)_b$ = 2.32, $\bar{d}(Cu\cdots Cu)$ = 3.33 Å.

Reaction of copper(II) ionic liquids with mercury

Because the dominant form of mercury in natural gas is elemental, tests were conducted to determine the solubility of Hg(0) in the ionic liquids by heating a droplet of mercury (Sigma Aldrich) with the ionic liquids at 60 °C overnight in a sealed vial. No precautions to exclude air were made during sample loading. In each case, a colour change was observed in the ionic liquid, with the characteristic brown colour of the chlorocuprate(II)-based systems changing to (i) a clear pale green ionic liquid at χ_{CuCl_2} = 0.33, or to (ii) a pale orange-yellow ionic liquid with precipitation of a pale grey-white solid at χ_{CuCl_2} = 0.50, as shown in Fig. 3. After heating, the size of the mercury drops remaining in the vials had visibly reduced and the mercury content in ionic liquid phase was determined by mercury analysis. The results are shown in Table 2.

Over 15 wt% mercury dissolution was observed (Table 2) for each of the chlorocuprate(II) ionic liquids tested, as determined from the water soluble mercury content of diluted aliquots of the ionic liquids. Reactive dissolution with similar end results was observed for the ionic liquids prepared from anhydrous and hydrated copper(II) chloride. A similar ability to dissolve mercury was observed for both χ_{CuCl_2} = 0.33 and 0.50, although the apparent outcomes of the dissolution process appear to be slightly different. The amount of mercury that was solubilised by the ionic liquids can be expressed by the molar concentration ratio $[Cu(II)_{IL}] : [Hg(II)_{IL}]$ (in Table 2) from the initial concentration of copper in the ionic liquids and mass of mercury extracted. In all cases, a small excess of unreacted copper(II) in solution was apparent due to the residual paler brown colouration. This would imply that one

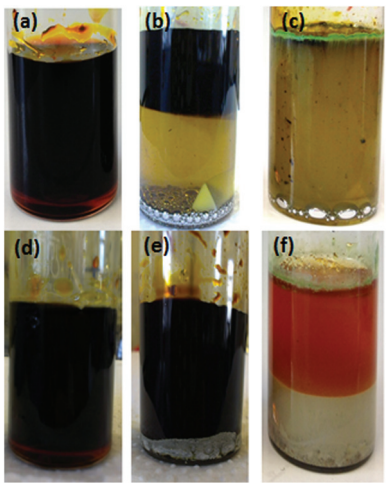

Fig. 3 The reaction of an excess of liquid mercury with 1-butyl-3-methylimidazolium chlorocuprate(II) ionic liquids at 60 °C. The top three photographs correspond to χ_{CuCl_2} = 0.33 and the bottom three to χ_{CuCl_2} = 0.50. At χ_{CuCl_2} = 0.33, (a) the initial ionic liquid mixture transforms to (b), a partially decolourised solution after mixing with Hg(0) for 5 min and then to (c) after extended mixing. At χ_{CuCl_2} = 0.50, (d) the initial ionic liquid mixture transforms through (e) after mixing with Hg(0) for 5 min to (f), a clear, largely decolourised ionic liquid phase containing a fine, grey-white precipitate after extended mixing.

Table 2 Solubility of bulk elemental mercury in metal-containing ionic liquid system at 60 °C (averages of three measurements)

Ionic liquid composition	wt% mercury dissolved in IL	$[Cu(II)_{IL}]$: $[Hg(II)_{IL}]$
$[C_4mim]Cl–CuCl_2·2H_2O$ (1 : 1)	22.1 ± 1.4	2.6
$[C_2mim]Cl–CuCl_2$ (2 : 1)	21.3 ± 2.3	2.2
$[N_{4\,4\,4\,1}]Cl–CuCl_2$ (2 : 1)	15.9 ± 0.3	2.4
$[N_{4\,4\,4\,1}]Cl–CuCl_2·2H_2O$ (2 : 1)	15.2 ± 0.1	2.3
[Chol]Cl–EG–$CuCl_2·2H_2O$ (1 : 2 : 1)[a]	16.9 ± 0.1	3.0

[a] Chol = cholinium; EG = diethylene glycol.

mole of mercury was required to reduce two moles of copper:

$$Hg(0) + 2Cu(II) \rightarrow Hg(II) + 2Cu(I)$$

The simplest mechanisms that can be proposed for this reaction, depending on the stoichiometry of the chlorocuprate(II) ionic liquids, are shown in eqn (1)–(3).

$$2[CuCl_4]^{2-} + Hg(0) \rightarrow [HgCl_4]^{2-} + 2[CuCl_2]^{-} \quad (1)$$

$$2[Cu_2Cl_6]^{2-} + 2Hg(0) \rightarrow [Hg_2Cl_6]^{2-} + 2[CuCl_2]^{-} + 2CuCl(s) \quad (2)$$

$$[Cu_2Cl_6]^{2-} + Hg(0) \rightarrow HgCl_2(s) + 2[CuCl_2]^{-} \quad (3)$$

The changes in colour of the copper(II)-containing ionic liquids after reaction with mercury are consistent with reduction to copper(I). Bolkan and Yoke,[33] described copper(I) systems ([C_2mim]Cl–CuCl; 0.33 < χ_{CuCl} < 0.67) as having colours that varied from pale yellow to light green with increasing χ_{CuCl}, and that darken rapidly in air and become paramagnetic as copper(II) is formed.

In eqn (1), all the products are anionic, and will incorporate into the ionic liquid. eqn (2) and (3) represent two contrasting interpretations of the observed reaction. In eqn (2), copper(I) chloride precipitates and in eqn (3), mercury(II) chloride precipitates. In the former case, the remaining solution contains both mercury(II) and copper(I) species; in the latter case, there will be no mercury in solution.

In eqn (2), it is speculated that the speciation of mercury is $[Hg_2Cl_6]^{2-}$. There is no evidence that this would be the speciation as it may be a monomeric species[34] or a polymeric species,[35] but the balance of probability is that it is likely to be dimeric.[36] Whatever the speciation, it does not affect the validity of the following arguments.

Examples of ^{199}Hg NMR spectra taken from {[C_4mim]Cl–$CuCl_2$ (χ_{CuCl_2} = 0.50) + Hg(0)} and {[C_4mim]Cl–$CuCl_2$ (χ_{CuCl_2} = 0.33) + Hg(0)} systems are shown in Fig. 4. Well defined ^{199}Hg NMR signals were obtained in each case, but with different chemical shifts. For χ_{CuCl_2} = 0.33, this peak was found at −1106 ppm (relative to 1 M $HgCl_2$ in dmso); for χ_{CuCl_2} = 0.50, the peak appeared at −1140 ppm. These positions are consistent with the formation of chloromercurate(II) anions,[37] where the mercury is in the environment of four chlorine atoms. The lower field peak is assigned to $[HgCl_4]^{2-}$ and the higher peak

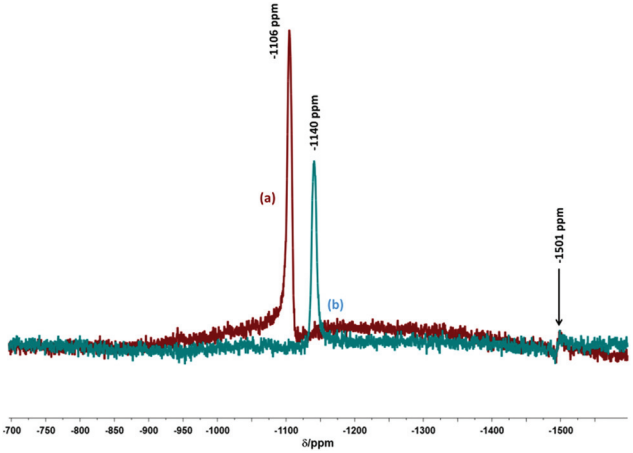

Fig. 4 ^{199}Hg NMR (23 °C, neat, 89.57 MHz) spectra of the ionic liquids obtained from the reaction mixtures of (a) $[C_4mim]_2[CuCl_4]$ + Hg(0) (red trace) and (b) $[C_4mim]_2[Cu_2Cl_6]$ + Hg(0) (blue trace). The peak at −1501 ppm is the reference peak.

to $[Hg_2Cl_6]^{2-}$. As it is known that $[HgCl_3]^{-}$ has a peak at −1197 ppm,[40] this suggests that the mercury complex anion formed is dimeric rather than monomeric. This provides strong support for the reaction schemes outlined in eqn (1) and (2). Eqn (3) has been eliminated as it would imply the absence of mercury in solution. The formation of a precipitate from the reaction of liquid mercury with the [C_4mim]Cl–$CuCl_2$ (χ_{CuCl_2} = 0.50) ionic liquid combined with the presence of chloromercurate(II) anions in solution as shown from ^{199}Hg NMR spectroscopy supports the reaction mechanism in eqn (2) at this composition and the precipitation of CuCl as the reaction shifts the ionic liquid towards chloride deficient, *i.e. acidic*, compositions. While little is known about the phase behaviour of chloromercurate(II) ionic liquids with χ_{HgCl_2},[38,39] the limiting point for homogeneity in chlorocuprate(I) systems is χ_{CuCl} = 0.67,[34] that is, with the copper : chloride ratio of 2 : 3.

Copper(II) supported ionic liquids in the laboratory

The above results from the reactions of the copper(II) ionic liquids with elemental mercury give a good indication that they might be the basis of an absorption scrubber. This would combine the thermodynamically favourable oxidation of mercury(0) to mercury(II) by the copper(II), followed by complexation (and hence stabilisation) by the liberated chloride ions. Although in the laboratory, it is clearly possible to develop a mercury scrubber based on an ionic liquid system in the fluid state, the efficiency of passing natural gas through a viscous liquid system would prevent its scale-up for an industrial process. The logical way forward was to coat a dispersed solid with a selected and optimised ionic liquid to form a class of materials now recognised as a supported ionic liquid phase (SILP).[25] This would lead to good contact between the gas and the ionic liquid, high throughput flow, and mechanical strength. A typical SILP is shown in Fig. 5.

Further, most mercury removal units used in the oil and gas industry are fixed-bed scrubbers, and so a SILP approach

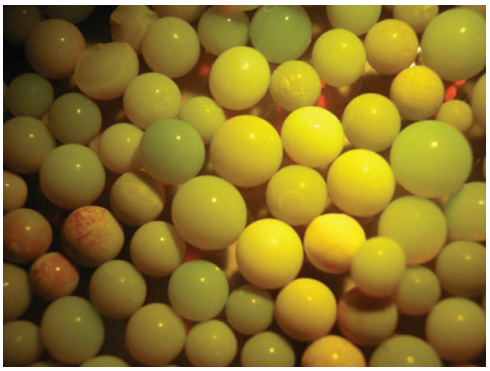

Fig. 5 An example of a SILP containing chlorocuprate(II) ionic liquid impregnated porous 4 mm diameter silica spheres.

to heterogenise the ionic liquids would be a natural fit with standard industrial practice. SILPs, which incorporate high surface area thin-films of ionic liquids within a porous solid scaffold, have many advantages for efficient gas–liquid contacting when a static liquid phase (*i.e.* as a catalyst or adsorbent) is required.[25]

SILPs containing the chlorocuprate(II) ionic liquids at 10 wt% loading were prepared by the incipient wetness method, adding solutions of the respective ionic liquids in methanol to porous silica beads, followed by drying overnight at 80 °C. After drying, the SILPs were orange-yellow (see Fig. 5), in contrast to the characteristic green of the methanolic solutions of the copper salts. ATIR spectra of SILPs showed no vibrational bands that could be assigned to methanol or to water, other than that residual on the silica surface (Fig. 6).

Mercury adsorption from gas streams was tested by passing a mercury-containing gas (either N_2 or CH_4) through a fixed bed of adsorbent, and comparing the inlet and outlet mercury concentrations. The more efficient the adsorbent is at

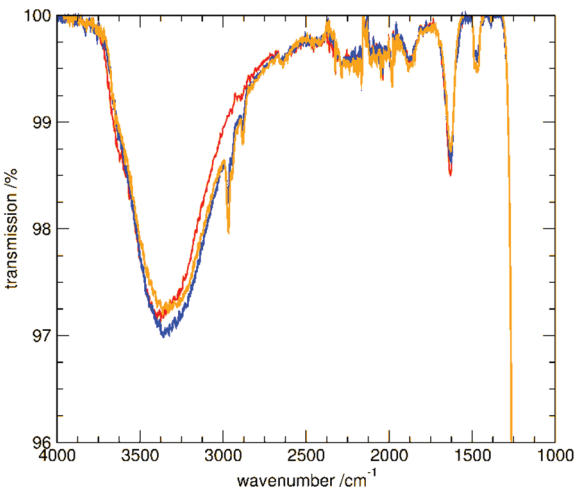

Fig. 6 ATR IR spectra comparing a silica support (red) and SILPs prepared with overnight drying at 80 °C (blue) or drying *in vacuo* (orange), illustrating the absence of additional –OH stretching frequencies in the SILPS that could be attributable to methanol or water. Peaks at 2965 and 2882 cm^{-1} derive from the ionic liquid cation.

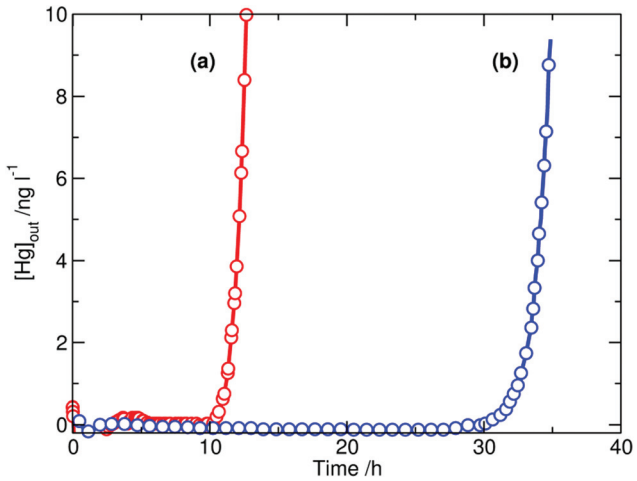

Fig. 7 Mercury breakthrough curves for the capture of mercury vapour from dinitrogen gas ([Hg]$_{in}$ = 2000 ng l^{-1}, flow rate = 600 cm^3 min^{-1}, T = 25 °C) using 0.10 g samples of (a) a sulfur-impregnated activated carbon and of (b) a 10 wt% [N_{4441}]Cl–$CuCl_2$ (χ_{CuCl_2} = 0.50) SILP on porous silica (135 m^2 g^{-1} surface area and 0.83 cm^3 g^{-1} pore volume). Similar results were obtained using methane as the carrier gas.

removing mercury from the gas, the longer the time it takes for mercury to be detected at the outlet. The time from injection to detection is defined as the breakthrough time. Over the course of the measurements, the inlet mercury concentration was held at the high level of 2000 ng l^{-1} in order to accelerate the breakthrough tests. In packed adsorbent beds with no channelling, the outlet mercury concentration follows the ideal (and observed) profile illustrated in Fig. 7. The outlet concentration remained constant at less than 0.2 ng l^{-1} prior to breakthrough, which was characterised by a rapid increase in its concentration. The breakthrough time was defined as the time at which mercury capture from the gas stream decreased to below 99.5% capture efficiency ([Hg]$_{out}$ > 10 ng l^{-1}). Characteristic mercury outlet profiles obtained under test conditions for a sulfur-impregnated activated carbon (*ca.* 10 wt% sulfur) and for a chlorocuprate(II) containing SILP (10 wt% [$N_{4\,4\,4\,1}$]Cl–$CuCl_2$, χ_{CuCl_2} = 0.50 on porous silica, 135 m^2 g^{-1} surface area and 0.83 cm^3 g^{-1} pore volume) are shown in Fig. 7.

Under the conditions defined in Fig. 7, the selected SILP remained active for 35 h until breakthrough, which corresponded to a mercury uptake of *ca.* 2.5 wt% (2.52 mg, 1.27 × 10^{-5} mol). This 100 mg SILP sample contained 2.71 × 10^{-5} moles of copper(II), and so the breakthrough point represents 93% mercury capture efficiency based on the proposed capture mechanism requiring oxidation by two copper(II) centres. The activated carbon, in contrast, showed poorer performance, with a breakthrough of 12.7 h, which is equivalent to 0.9 wt% mercury capture on the support. This was lower than anticipated, although this may be due to the extremely short residence times in these accelerated screening tests. Thus, in a laboratory test rig, the SILP outperformed the activated carbon by a factor of 3, which was very encouraging for moving from laboratory to pilot plant.

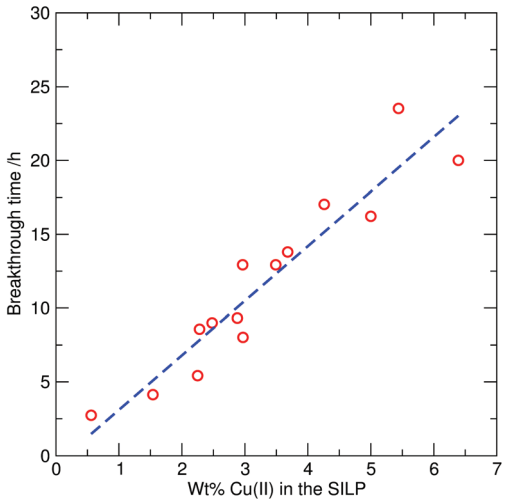

Fig. 8 The change in mercury breakthrough time for SILPs containing different cations ($[N_{4\ 4\ 4\ 1}]^+$, $[C_2mim]^+$, and $[C_4mim]^+$) as a function of ionic liquid loading in the SILP, expressed as wt% copper. Compared to the results shown in Fig. 7, the experimental sample sizes here are reduced to 30 mg, with all other conditions identical ($[Hg]_{in}$ = 2000 ng l^{-1}, flow rate = 600 cm^3 min^{-1}, T = 25 °C), which results in a corresponding decrease in the breakthrough time.

Ionic liquids containing different cations ($[N_{4\ 4\ 4\ 1}]^+$, $[C_2mim]^+$, and $[C_4mim]^+$) were tested, resulting in similar breakthrough performance which appears to correlate with the total amount copper(II) within the tested samples (Fig. 8). At higher loadings, a reduction in mercury capture performance was observed, presumably through plugging of the support through pore filling. This could be partially alleviated by changing to supports with large pore geometries.

After exhaustive extraction in contact with mercury-containing gas streams, the SILPs change colour from orange to pale green. This transformation is comparable to the colour changes observed after reaction of the neat ionic liquids with liquid mercury (Fig. 5). As a useful laboratory application, Fig. 9 shows a bed of chlorocuprate(II)-containing SILP used as a mercury trap on the off-gas line from a PSA Sir Galahad mercury analyser in our laboratory. The mercury breakthrough front can be clearly seen at the sharp transition from spent (pale green) absorbent to active (yellow-orange) material.

Interestingly, Haumann and co-workers[40] have also recently reported the use of chlorocuprate(II)-containing SILPs for gas absorption applications. They investigated ammonia capture from air taking advantage of the strong coordination of nucleophilic amines to copper, and suggested their potential uses in broadband filters for breathing apparatus.

Copper(II) supported ionic liquids at scale

The laboratory results demonstrated that efficient and comprehensive scrubbing of mercury vapour from gas streams could be achieved with excellent capture kinetics. The accelerated breakthrough screening used residence times in the order of 50 ms in the test rig, and breakthrough times correlated with theoretical maximum mercury capacities based on the mechanisms detailed in eqn (1) and (2). Following on from these small-scale laboratory tests, larger batches (*ca.* 100 g) of chlorocuprate(II) SILPs were prepared and tested in a 200 cm^3 pilot-scale slipstream scrubber on-site at a Gas Processing Plant in Malaysia. The pilot trials (over 60 days) yielded a gas stream with mercury outlet concentrations of <0.01 μg m^{-3} (Fig. 10), at least one order of magnitude below the sales specification for the natural gas.

This allowed a smooth transition to full plant implementation using 30 m^3 of a SILP (see Fig. 11). After three years of continuous operation, the outlet mercury concentration from the plant remained low, meeting the plant outlet specifications. This represents a remarkable success of transferring laboratory chemistry to full scale plant operation in a remarkably fast implementation (less than four years). The SILP is now commercialised *via* a marketing licensing agreement between PETRONAS and Clariant.[41]

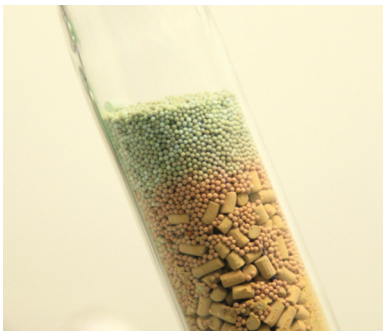

Fig. 9 Example of a chlorocuprate(II)-containing SILP used as a mercury trap on the off-gas line from a PSA Sir Galahad mercury analyser in our laboratory. The mercury breakthrough front can be clearly seen at the sharp transition from spent (pale green) to active (yellow-orange) absorbent. The packed bed contains ionic liquid impregnated on two different silica supports; spherical beads and extrudates.

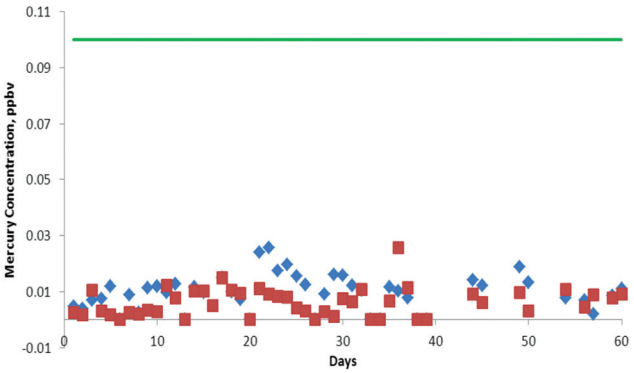

Fig. 10 Results from a pilot trial (over 60 days) of a copper(II) containing SILP in a slipstream scrubber (200 cm^3) for mercury removal from natural gas on-site at a Gas Processing Plant in Malaysia, showing the mercury outlet concentrations after passing through commercial material (blue diamonds) and SILPs (red squares). The average extraction efficiency was 99.998%. The green line indicates specification for sales quality gas (0.1 μg m^{-3} mercury).[27]

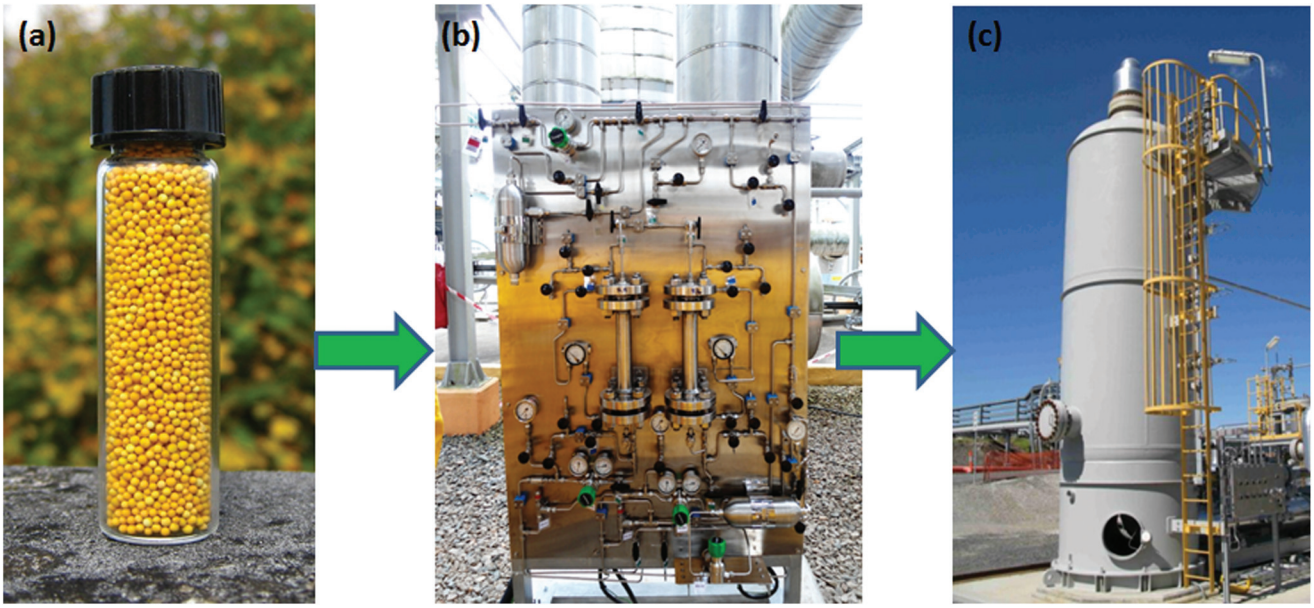

Fig. 11 Transformation from (a) lab-scale preparation of chlorocuprate(II) SILPs through to (b) pilot-scale using 100 cm^3 of SILP on production plant gas feeds to (c) full-scale mercury removal units with 20 m^3 of SILP at a gas processing plant site.[27]

Conclusions

We have demonstrated that it is possible to develop in the laboratory, processes with industrial applicability. Starting at the gram scale, the translation of the ionic liquid chemistry into a SILP material that was scaled to full industrial implementation within four years has been exemplified. The fundamental chemistry (namely oxidative dissolution and complexation of mercury into the ionic liquid as a stable anionic mercurate(II) species) does not change with the scale of the process and the ability to digest large quantities of mercury (up to 20 wt%), coupled with efficient gas-contacting, made possible by formation of a SILP, underpins the successful development of these materials as commercially competitive solid phase mercury adsorbents in the natural gas industry.

Acknowledgements

We are indebted to our many colleagues at PETRONAS for their funding and discussions about this work. We would also like thank Chemviron Carbon, Ltd. for supplying activated carbon samples for testing, and thank the EPSRC UK National Crystallography Service at the University of Southampton for the collection of the crystallographic data.[42]

Notes and references

1 C. T. Driscoll, R. P. Mason, H. M. Chan, D. J. Jacob and N. Pirrone, *Environ. Sci. Technol.*, 2013, **47**, 4967–4983.
2 G. Liu, Y. Cai, N. O'Driscoll, X. Feng and G. Jiang, Overview of Mercury in the Environment, in *Environmental Chemistry and Toxicology of Mercury*, ed. G. Liu, Y. Cai and N. O'Driscoll, John Wiley & Sons, Hoboken, New Jersey, 2011, pp. 1–12.
3 S. M. Wilhelm and N. Bloom, *Fuel Process. Technol.*, 2000, **63**, 1–27.
4 United Nations Environment Programme, *Global Mercury Assessment and Environmental Transport*, UNEP Chemicals Branch, Geneva, Switzerland, 2013, ISBN: 978-92-807-3310-5.
5 S. M. Wilhelm, *Process Saf. Prog.*, 2009, **28**, 259–266.
6 G. T. Kinney, *Oil Gas J.*, 1975, 192.
7 E. J. Granite, H. W. Pennline and R. A. Hargis, *Ind. Eng. Chem. Res.*, 2000, **39**, 1020–1029; N. Eckersley, *Hydrocarb. Process*, 2012, 29–35.
8 W. Liu, R. D. Vidić and T. D. Brown, *Environ. Sci. Technol.*, 1998, **32**, 531–538.
9 R. D. Vidić and D. P. Siler, *Carbon*, 2001, **39**, 3–14.
10 W. Du, L. Yin, Y. Zhuo, Q. Xu, L. Zhang and C. Chen, *Ind. Eng. Chem. Res.*, 2014, **53**, 582–591.
11 See for example: M. Freemantle, *An Introduction to Ionic Liquids*, Royal Society of Chemistry, Cambridge, 2010; N. V. Plechkova and K. R. Seddon, *Chem. Soc. Rev.*, 2008, **37**, 123–150; J. P. Hallett and T. Welton, *Chem. Rev.*, 2011, **111**, 3508–3576.
12 M. V. Mancini, N. Spreti, P. Di Profio and R. Germani, *Sep. Purif. Technol.*, 2013, **116**, 294–299.
13 A. E. Visser, R. P. Swatloski, W. M. Reichert, R. Mayton, S. Sheff, A. Wierzbicki, J. H. Davis Jr. and R. D. Rogers, *Chem. Commun.*, 2001, 135–136.
14 A. E. Visser, R. P. Swatloski, S. T. Griffin, D. H. Hartman and R. D. Rogers, *Sep. Sci. Technol.*, 2001, **36**, 785–804.
15 N. Papaiconomou, J. M. Lee, J. Salminen, M. von Stosch and J. M. Prausnitz, *Ind. Eng. Chem. Res.*, 2008, **47**, 5080–5086.

16 L. Ji, S. W. Thiel and N. G. Pinto, *Ind. Eng. Chem. Res.*, 2008, **47**, 8396–8400; L. Ji, M. Abu-Daabes and N. G. Pinto, *Chem. Eng. Sci.*, 2009, **64**, 486–491.
17 R. D. Rogers and J. D. Holbrey, *World Pat. Appl*, WO2010116167, 2010.
18 Y. Sasson, M. Chidambaram and Z. Barnea, *US Pat*, US8101144, 2012; Z. Barnea, T. Sachs, M. Chidambaram and Y. Sasson, *J. Hazard. Mater.*, 2013, **244**, 495–500.
19 M. Fields, G. V. Hutson, K. R. Seddon and C. M. Gordon, *World Pat. Appl*, WO9806106, 1998.
20 P. Nockemann, B. Thijs, S. Pittois, J. Thoen, C. Glorieux, K. Van Hecke, L. Van Meervelt, B. Kirchner and K. Binnemans, *J. Phys. Chem. B*, 2006, **110**, 20978–20992.
21 J. D. Holbrey, I. Lopez-Martin, G. Rothenberg, K. R. Seddon, G. Silvero and X. Zheng, *Green Chem.*, 2008, **10**, 87–92.
22 J. Estager, J. D. Holbrey and M. Swadźba-Kwaśny, *Chem. Soc. Rev.*, 2014, **43**, 847–886.
23 M. Y. Lui, L. Crowhurst, J. P. Hallett, P. A. Hunt, H. Niedermeyer and T. Welton, *Chem. Sci.*, 2011, **2**, 1491–1496.
24 M. Abai, M. Atkins, K. Y. Cheun, J. D. Holbrey, P. Nockemann, K. R. Seddon, G. Srinivasan and Y. Zou, *World Pat. Appl*, WO2012046057, 2012.
25 *Supported Ionic Liquids: Fundamentals and Applications*, ed. R. Fehrmann, A. Riisager and M. Haumann, Wiley, Weinheim, 2014.
26 M. Abai, M. P. Atkins, A. Hassan, J. D. Holbrey, Y. Kuah, P. Nockemann, A. A. Oliferenko, N. V. Plechkova, S. Rafeen, A. A. Rahman, K. R. Seddon, S. M. Shariff, G. Srinivasan and Y. Zou, International Gas Union Research Conference 2011, Seoul, Korea, 2011, http://members.igu.org/old/IGU%20Events/igrc/igrc2011/igrc-2011-proceedings-and-presentations/poster-papers-session-4/P4-26_Martin%20Atkins.pdf.
27 R. E. Taylor and F. P. Gabbaï, *J. Mol. Struct.*, 2007, **839**, 28–32.
28 O. V. Dolomanov, L. J. Bourhis, R. J. Gildea, J. A. K. Howard and H. Puschmann, *J. Appl. Crystallogr.*, 2009, **42**, 339–341.
29 G. M. Sheldrick, *Acta Crystallogr., Sect. A: Fundam. Crystallogr.*, 2008, **64**, 112–122.
30 A. P. Abbott, K. El Ttaib, G. Frisch, K. J. McKenzie and K. S. Ryder, *Phys. Chem. Chem. Phys.*, 2009, **11**, 4269–4277.
31 G. Li, D. M. Camaioni, J. E. Amonette, Z. C. Zhang, T. J. Johnson and J. L. Fulton, *J. Phys. Chem. B*, 2010, **114**, 12614–12622.
32 D. W. Smith, *Coord. Chem. Rev.*, 1976, **21**, 93–158; R. D. Willett and U. Geiser, *Inorg. Chem.*, 1986, **25**, 4558–4561; P. De Vreese, N. R. Brooks, K. Van Hecke, L. Van Meervelt, E. Matthijs, K. Binnemans and R. Van Deun, *Inorg. Chem.*, 2012, **51**, 4972–4981.
33 S. A. Bolkan and J. T. Yoke, *Inorg. Chem.*, 1986, **25**, 3587–3590.
34 P. Nockemann and G. Meyer, *Z. Anorg. Allg. Chem.*, 2003, **629**, 123–128.
35 M. Rademeyer, D. G. Billing and A. Lemmerer, *Acta Crystallogr., Sect. E: Struct. Rep. Online*, 2006, **62**, m1716–m1718; A. Linden, B. D. James, J. Liesegang and N. Gonis, *Acta Crystallogr., Sect. B: Struct. Sci.*, 1999, **55**, 396–409.
36 P. Nockemann and G. Meyer, *Acta Crystallogr., Sect. E: Struct. Rep. Online*, 2002, **58**, m534–m536.
37 R. E. Taylor, S. Bai and C. Dybowski, *J. Mol. Struct.*, 2011, **987**, 193–198; G. Klose, F. Volke, G. Peinel and G. Knobloch, *Magn. Reson. Chem.*, 1993, **31**, 548–551.
38 A. Metlen, B. Mallick, R. W. Murphy, A.-V. Mudring and R. D. Rogers, *Inorg. Chem.*, 2013, **52**, 13997–14009.
39 B. Mallick, A. Metlen, M. Nieuwenhuyzen, R. D. Rogers and A. V. Mudring, *Inorg. Chem.*, 2012, **51**, 193–200.
40 F. T. U. Kohler, S. Popp, H. Klefer, I. Eckle, C. Schrage, B. Böhringer, D. Roth, M. Haumann and P. Wasserscheid, *Green Chem.*, 2014, **16**, 3560–3568.
41 Clariant Newsroom, 'Clariant And Petronas Sign Licensing Collaboration', http://newsroom.clariant.com/clariant-and-petronas-sign-licensing-collaboration/, 2014.
42 S. J. Coles and P. A. Gale, *Chem. Sci.*, 2012, **3**, 683–689.

